

---

# SOLAR AND STELLAR MAGNETIC ACTIVITY

---

C. J. SCHRIJVER

*Stanford-Lockhead Institute for Space Research, Palo Alto*

C. ZWAAN

*Astronomical Institute, University of Utrecht*



**CAMBRIDGE**  
UNIVERSITY PRESS

PUBLISHED BY THE PRESS SYNDICATE OF THE UNIVERSITY OF CAMBRIDGE  
The Pitt Building, Trumpington Street, Cambridge, United Kingdom

CAMBRIDGE UNIVERSITY PRESS  
The Edinburgh Building, Cambridge CB2 2RU, UK <http://www.cup.cam.ac.uk>  
40 West 20th Street, New York, NY 10011-4211, USA <http://www.cup.org>  
10 Stamford Road, Oakleigh, Melbourne 3166, Australia  
Ruiz de Alarcón 13, 28014 Madrid, Spain

© Cambridge University Press 2000

This book is in copyright. Subject to statutory exception  
and to the provisions of relevant collective licensing agreements,  
no reproduction of any part may take place without  
the written permission of Cambridge University Press.

First published 2000

Printed in the United States of America

Typeface Times Roman 10.5/12.5 pt. and Gill Sans System L<sup>A</sup>T<sub>E</sub>X 2<sub>ε</sub> [TB]

*A catalog record for this book is available from the British Library.*

*Library of Congress Cataloging in Publication Data*

Schrijver, Carolus J.

Solar and stellar magnetic activity / Carolus J. Schrijver,  
Cornelis Zwaan.

p. cm. – (Cambridge astrophysics series ; 34)

ISBN 0-521-58286-5 (hc.)

1. Solar magnetic fields. 2. Stars – Magnetic fields. I. Zwaan,  
Cornelis. II. Title. III. Series.

QB539.M23S37 1999  
523.7'2 – dc21

99-21364  
CIP

ISBN 0 521 58286 5 hardback



---

# Contents

---

|                              |                  |
|------------------------------|------------------|
| <i>List of Illustrations</i> | <i>page xii</i>  |
| <i>List of Tables</i>        | <i>page xv</i>   |
| <i>Preface</i>               | <i>page xvii</i> |

|   |            |
|---|------------|
| <b>1 Introduction: solar features and terminology</b>     | <b>1</b>   |
| <b>2 Stellar structure</b>                                | <b>10</b>  |
| 2.1 Global stellar structure                              | 10         |
| 2.2 Convective envelopes: classical concepts              | 14         |
| 2.3 Radiative transfer and diagnostics                    | 19         |
| 2.4 Stellar classification and evolution                  | 38         |
| 2.5 Convection in stellar envelopes                       | 45         |
| 2.6 Acoustic waves in stars                               | 60         |
| 2.7 Basal radiative losses                                | 65         |
| 2.8 Atmospheric structure not affected by magnetic fields | 70         |
| <b>3 Solar differential rotation and meridional flow</b>  | <b>73</b>  |
| 3.1 Surface rotation and torsional patterns               | 74         |
| 3.2 Meridional and other large-scale flows                | 77         |
| 3.3 Rotation with depth                                   | 79         |
| <b>4 Solar magnetic structure</b>                         | <b>82</b>  |
| 4.1 Magnetohydrodynamics in convective envelopes          | 83         |
| 4.2 Concentrations of strong magnetic field               | 92         |
| 4.3 Magnetohydrostatic models                             | 98         |
| 4.4 Emergence of magnetic field and convective collapse   | 105        |
| 4.5 Omega loops and toroidal flux bundles                 | 108        |
| 4.6 Weak field and the magnetic dichotomy                 | 110        |
| <b>5 Solar magnetic configurations</b>                    | <b>115</b> |
| 5.1 Active regions  | 115        |
| 5.2 The sequence of magnetoconvective configurations      | 126        |
| 5.3 Flux positioning and dynamics on small scales         | 126        |

|           |   |            |
|-----------|---|------------|
| 5.4       | The plage state   | 132        |
| 5.5       | Heat transfer and magnetic concentrations               | 137        |
| <b>6</b>  | <b>Global properties of the solar magnetic field</b>    | <b>138</b> |
| 6.1       | The solar activity cycle                                | 138        |
| 6.2       | Large-scale patterns in flux emergence                  | 143        |
| 6.3       | Distribution of surface magnetic field                  | 155        |
| 6.4       | Removal of magnetic flux from the photosphere           | 167        |
| <b>7</b>  | <b>The solar dynamo</b>                                 | <b>173</b> |
| 7.1       | Mean-field dynamo theory                                | 174        |
| 7.2       | Conceptual models of the solar cycle                    | 178        |
| 7.3       | Small-scale magnetic fields                             | 182        |
| 7.4       | Dynamos in deep convective envelopes                    | 184        |
| <b>8</b>  | <b>The solar outer atmosphere</b>                       | <b>186</b> |
| 8.1       | Topology of the solar outer atmosphere                  | 186        |
| 8.2       | The filament-prominence configuration                   | 197        |
| 8.3       | Transients  | 199        |
| 8.4       | Radiative and magnetic flux densities                   | 209        |
| 8.5       | Chromospheric modeling                                  | 217        |
| 8.6       | Solar coronal structure                                 | 220        |
| 8.7       | Coronal holes   | 227        |
| 8.8       | The chromosphere–corona transition region               | 229        |
| 8.9       | The solar wind and the magnetic brake                   | 231        |
| <b>9</b>  | <b>Stellar outer atmospheres</b>                        | <b>238</b> |
| 9.1       | Historical sketch of the study of stellar activity      | 238        |
| 9.2       | Stellar magnetic fields                                 | 238        |
| 9.3       | The Mt. Wilson Ca II HK project                         | 242        |
| 9.4       | Relationships between stellar activity diagnostics      | 246        |
| 9.5       | The power-law nature of stellar flux–flux relationships | 252        |
| 9.6       | Stellar coronal structure                               | 258        |
| <b>10</b> | <b>Mechanisms of atmospheric heating</b>                | <b>266</b> |
| <b>11</b> | <b>Activity and stellar properties</b>                  | <b>277</b> |
| 11.1      | Activity throughout the H–R diagram                     | 277        |
| 11.2      | Measures of atmospheric activity                        | 281        |
| 11.3      | Dynamo, rotation rate, and stellar parameters           | 283        |
| 11.4      | Activity in stars with shallow convective envelopes     | 291        |
| 11.5      | Activity in very cool main-sequence stars               | 294        |
| 11.6      | Magnetic activity in T Tauri objects                    | 296        |
| 11.7      | Long-term variability of stellar activity               | 299        |

|   |            |
|---|------------|
| <i>Contents</i>   | <b>xi</b>  |
| <b>12 Stellar magnetic phenomena</b>                        | <b>303</b> |
| 12.1 Outer-atmospheric imaging                              | 303        |
| 12.2 Stellar plages, starspots, and prominences             | 305        |
| 12.3 The extent of stellar coronae                          | 310        |
| 12.4 Stellar flares   | 312        |
| 12.5 Direct evidence for stellar winds                      | 314        |
| 12.6 Large-scale patterns in surface activity               | 318        |
| 12.7 Stellar differential rotation                          | 319        |
| <br>  |            |
| <b>13 Activity and rotation on evolutionary time scales</b> | <b>324</b> |
| 13.1 The evolution of the stellar moment of inertia         | 324        |
| 13.2 Observed rotational evolution of stars                 | 326        |
| 13.3 Magnetic braking and stellar evolution                 | 329        |
| <br>  |            |
| <b>14 Activity in binary stars</b>                          | <b>336</b> |
| 14.1 Tidal interaction and magnetic braking                 | 336        |
| 14.2 Properties of active binaries                          | 340        |
| 14.3 Types of particularly active stars and binary systems  | 342        |
| <br>  |            |
| <b>15 Propositions on stellar dynamos</b>                   | <b>344</b> |
| <br>  |            |
| <i>Appendix I: Unit conversions</i>                         | 351        |
| <i>Bibliography</i>   | 353        |
| <i>Index</i>  | 375        |

---

# List of Illustrations

---

|      |   |    |
|------|---|----|
| 1.1  | Full-disk solar images and magnetogram                                | 2  |
| 1.2  | Active-region image set   | 5  |
| 1.3  | H $\alpha$ filtergrams  | 8  |
| 2.1  | Solar convection-zone model   | 16 |
| 2.2  | Definitions of radiative intensity and of a plane-parallel atmosphere | 20 |
| 2.3  | Extinction coefficient in the solar photosphere                       | 24 |
| 2.4  | Coronal radiative loss function                                       | 27 |
| 2.5  | $I$ and $V$ profiles  | 31 |
| 2.6  | Ca II K profiles  | 36 |
| 2.7  | Hertzsprung–Russell diagrams  | 39 |
| 2.8  | Color–magnitude diagrams and MK classification                        | 40 |
| 2.9  | Mass–luminosity relation  | 41 |
| 2.10 | Evolutionary tracks   | 42 |
| 2.11 | Stellar parameters along the main sequence                            | 45 |
| 2.12 | CH band head image and magnetogram for granular scales                | 46 |
| 2.13 | Supergranular flow and cell pattern, on magnetogram                   | 47 |
| 2.14 | Size distribution for granulation and supergranulation                | 49 |
| 2.15 | Subsurface convection topology  | 55 |
| 2.16 | Voronoi tessellations of Poisson-distributed generator points         | 59 |
| 2.17 | Ca II H+K flux densities in a sample of cool stars                    | 66 |
| 2.18 | Mg II h+k basal flux densities  | 67 |
| 3.1  | Solar differential rotation   | 76 |
| 3.2  | Meridional flow   | 78 |
| 3.3  | Internal solar rotation rate  | 80 |
| 4.1  | Magnetic field in a stationary, cellular flow                         | 86 |
| 4.2  | Flux-tube concept   | 87 |
| 4.3  | Radiative time scale  | 90 |

| <i>List of Illustrations</i>   | <b>xiii</b> |
|--|-------------|
| 4.4 Sunspot and pores  | 94          |
| 4.5 Flux-tube model  | 99          |
| 4.6 Sunspot field  | 101         |
| 4.7 Emerging flux region   | 106         |
| 4.8 $\Omega$ loop  | 107         |
| 4.9 Orientation of an active region                                      | 107         |
| 4.10 Toroidal roots of a large bipolar active region                     | 109         |
| 4.11 Internetwork field  | 111         |
| 5.1 Facular flows in an emerging flux region                             | 116         |
| 5.2 Theoretical configuration for emerging flux tube                     | 118         |
| 5.3 High-resolution magnetogram  | 123         |
| 5.4 Histograms of fluxes contained in photospheric concentrations        | 128         |
| 5.5 The sensitivity of the plage perimeter to the threshold flux density | 132         |
| 5.6 Plage magnetic flux against plage area                               | 133         |
| 5.7 Abnormal granulation in a region with a high magnetic flux density   | 134         |
| 6.1 Comparison of activity indices                                       | 138         |
| 6.2 Sunspot number against time  | 140         |
| 6.3 Butterfly diagram  | 141         |
| 6.4 Nests in magnetograms  | 143         |
| 6.5 Sunspot nests  | 145         |
| 6.6 Compactness of sunspot nests   | 146         |
| 6.7 Composite nests  | 147         |
| 6.8 Size distribution of bipolar regions                                 | 148         |
| 6.9 Orientations of bipolar active regions                               | 149         |
| 6.10 Dynamo aspects  | 152         |
| 6.11 Magnetic flux arch  | 152         |
| 6.12 Examples of synoptic magnetograms                                   | 155         |
| 6.13 Time-dependent distribution function for $ \varphi $                | 156         |
| 6.14 Disk-averaged magnetic flux density through a sunspot cycle         | 156         |
| 6.15 Flux cancellation   | 166         |
| 6.16 Formation of a $\cup$ loop  | 168         |
| 6.17 Elimination of toroidal flux  | 169         |
| 6.18 Magnetic features streaming out from a spot across the moat         | 170         |
| 7.1 Solar $\alpha\Omega$ dynamo  | 176         |
| 8.1 Canopy supported by monopolar flux tubes                             | 186         |
| 8.2 Topology of the outer atmosphere                                     | 186         |
| 8.3 Solar corona as observed with NIXT at 64 Å (Fe XVI, Mg X)            | 188         |

**xiv**     *List of Illustrations*

|      |  |     |
|------|--|-----|
| 8.4  | White-light corona   | 191 |
| 8.5  | Solar corona as observed with TRACE at 171 Å (Fe IX/X)               | 195 |
| 8.6  | Development of a solar flare   | 204 |
| 8.7  | Dynamic spectrum of radio bursts                                     | 206 |
| 8.8  | Ca II K-line core intensity vs. magnetic flux density at 2.4''       | 208 |
| 8.9  | Ca II K line-core intensity vs. magnetic flux density at 14.4''      | 211 |
| 8.10 | C IV vs. magnetic flux densities for solar and stellar data          | 214 |
| 8.11 | SOHO/LASCO image of the outer solar corona                           | 232 |
| 8.12 | Weber–Davis solutions for the solar wind                             | 235 |
| 9.1  | Characteristic field strengths for cool stars                        | 240 |
| 9.2  | Wilson–Bappu effect  | 242 |
| 9.3  | The Ca II H+K emission from solar-neighborhood stars                 | 245 |
| 9.4  | Relationship between coronal and chromospheric excess fluxes         | 247 |
| 9.5  | Simulated relationships between surface-averaged flux densities      | 255 |
| 9.6  | Exponents for flux–flux relationships                                | 256 |
| 9.7  | Cumulative contributions in Ca II H+K and soft X-rays                | 256 |
| 9.8  | Stellar coronal emission-measure distributions                       | 259 |
| 10.1 | Potential-field extrapolation over mixed-polarity network            | 273 |
| 11.1 | Activity across H–R diagram  | 278 |
| 11.2 | Rotation vs. activity in main-sequence stars I                       | 285 |
| 11.3 | Rotation vs. activity in main-sequence stars II                      | 286 |
| 11.4 | Rotation vs. activity in young cluster stars                         | 287 |
| 11.5 | Magnetic flux and activity vs. rotation rate                         | 288 |
| 11.6 | Dynamo efficiency function vs. the fractional volume of the envelope | 292 |
| 11.7 | Flux–flux relations for T Tauri objects                              | 297 |
| 11.8 | Ca II HK, 25-yr records  | 300 |
| 11.9 | Distribution of chromospheric activity                               | 301 |
| 13.1 | Moments of inertia of evolving stars                                 | 325 |
| 13.2 | Moments of inertia of radiative core and convective envelope         | 326 |
| 13.3 | Evolution of rotation in young main-sequence stars                   | 327 |
| 13.4 | Rotation rates of a sample of LC III giants                          | 328 |
| 13.5 | Rotation rates of a sample of LC IV subgiants                        | 329 |
| 13.6 | Timescales for magnetic braking                                      | 333 |
| 14.1 | Equipotential surfaces in a binary system                            | 337 |
| 14.2 | Eccentricity–period diagram for main-sequence binaries               | 339 |
| 14.3 | Power-law parameterization for active single and binary stars        | 341 |

---

# List of Tables

---

|      |   |     |
|------|---|-----|
| 2.1  | Radiative losses from the solar atmosphere                          | 26  |
| 2.2  | Selected diagnostics for solar and stellar activity                 | 35  |
| 2.3  | Duration of H-fusion phases   | 44  |
| 2.4  | Convective scales in the solar photosphere                          | 48  |
| 2.5  | Dimensionless numbers   | 53  |
| 2.6  | Properties of photospheres of selected cool stars                   | 54  |
| 2.7  | List of basal flux densities in Mg II, Si II, C II, Si IV, and C IV | 68  |
| 3.1  | Solar differential rotation   | 75  |
| 5.1  | Active region sizes   | 115 |
| 5.2  | Scaling relationships for active regions                            | 133 |
| 6.1  | The rules of solar activity   | 139 |
| 6.2  | Diffusion coefficients for flux dispersal                           | 160 |
| 8.1  | Power-law exponents for relationships between solar intensities     | 215 |
| 9.1  | Power-law exponents of stellar flux–flux relationships              | 248 |
| 9.2  | Nomenclature of single cool stars and cool-star binary systems      | 249 |
| 9.3  | Stellar coronal electron densities                                  | 263 |
| 10.1 | Sources and mechanisms of nonradiative heating                      | 267 |

---

# Introduction: solar features and terminology

---

The Sun serves as the source of inspiration and the touchstone in the study of stellar magnetic activity. The terminology developed in observational solar physics is also used in stellar studies of magnetic activity. Consequently, this first chapter provides a brief illustrated glossary of nonmagnetic and magnetic features, as they are visible on the Sun in various parts of the electromagnetic spectrum. For more illustrations and detailed descriptions, we refer to Bruzek and Durrant (1977), Foukal (1990), Golub and Pasachoff (1997), and Zirin (1988).

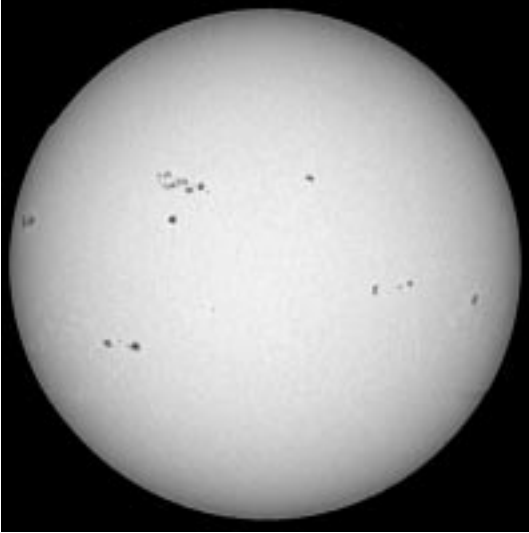
The *photosphere* is the deepest layer in the solar atmosphere that is visible in “white light” and in continuum windows in the visible spectrum. Conspicuous features of the photosphere are the *limb darkening* (Fig. 1.1a) and the *granulation* (Fig. 2.12), a time-dependent pattern of bright *granules* surrounded by darker *intergranular lanes*. These nonmagnetic phenomena are discussed in Sections 2.3.1 and 2.5.

The magnetic structure that stands out in the photosphere comprises dark *sunspots* and bright *faculae* (Figs. 1.1a and 1.2b). A large sunspot consists of a particularly dark *umbra*, which is (maybe only partly) surrounded by a less dark *penumbra*. Small sunspots without a penumbral structure are called *pores*. Photospheric faculae are visible in white light as brighter specks close to the limb.

The *chromosphere* is the intricately structured layer on top of the photosphere; it is transparent in the optical continuum spectrum, but it is optically thick in strong spectral lines. It is seen as a brilliantly purplish-red crescent during the first and the last few seconds of a total solar eclipse, when the moon just covers the photosphere. Its color is dominated by the hydrogen Balmer spectrum in emission. *Spicules* are rapidly changing, spikelike structures in the chromosphere observed beyond the limb (Fig. 4.7 in Bruzek and Durrant, 1977, or Fig. 9-1 in Foukal, 1990).

Chromospheric structure can always be seen, even against the solar disk, by means of monochromatic filters operating in the core of a strong spectral line in the visible spectrum or in a continuum or line window in the ultraviolet (see Figs. 1.1b, 1.1c, 1.2c and 1.3). In particular, filtergrams recorded in the red Balmer line  $H\alpha$  display a wealth of structure (Fig. 1.3). *Mottle* is the general term for a (relatively bright or dark) detail in such a monochromatic image. A strongly elongated mottle is usually called a *fibril*.

The photospheric granulation is a convective phenomenon; most other features observed in the photosphere and chromosphere are magnetic in nature. Sunspots, pores, and faculae are threaded by strong magnetic fields, as appears by comparing the magnetograms in Figs. 1.1 and 1.2 to other panels in those figures. On top of the photospheric



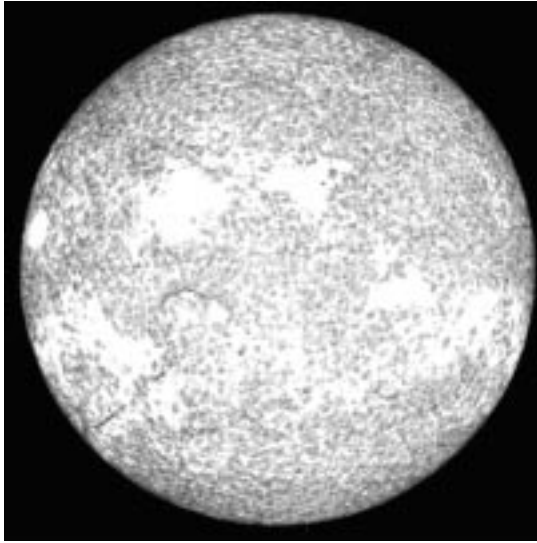
1.1 a

Fig. 1.1. Four faces of the Sun and a magnetogram, all recorded on 7 December 1991. North is to the top; West is to the right. Panel *a*: solar disk in white light; note the limb darkening. Dark sunspots are visible in the sunspot belt; the bright specks close to the solar limb are the photospheric *faculae* (NSO-Kitt Peak). Panel *b*: solar disk recorded in the Ca II K line core. Only the largest sunspots remain visible; bright *chromospheric faculae* stand out throughout the activity belt, also near the center of the disk. Faculae cluster in *plages*. In addition, bright specks are seen in the *chromospheric network*, which covers the Sun everywhere outside sunspots and plages (NSO-Sacramento Peak). Panel *c*: solar disk recorded in the H $\alpha$  line core. The plages are bright, covering also the sunspots, except the largest. The dark ribbons are called *filaments* (Observatoire de Paris-Meudon). Panel *d*: the solar *corona* recorded in soft X-rays. The bright *coronal condensations* cover the active regions consisting of sunspot groups and faculae. Note the intricate structure, with loops. Panel *e*: magnetogram showing the longitudinal (line-of-sight) component of the magnetic field in the photosphere; light gray to white patches indicate positive (northern) polarity, and dark gray to black ones represent negative (southern) polarity. Note that the longitudinal magnetic signal in plages and network decreases toward the limb (NSO-Kitt Peak).

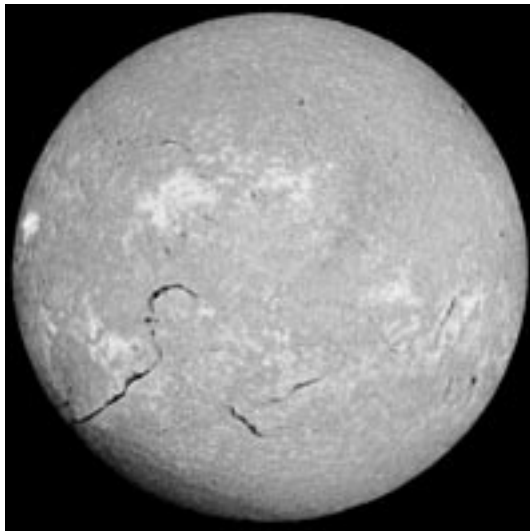
faculae are the *chromospheric faculae*, which are well visible as bright fine mottles in filtergrams obtained in the Ca II H or K line (Fig. 1.1*b*) and in the ultraviolet continuum around 1,600 Å (Fig. 1.2*c*). Whereas the faculae in “white light” are hard to see near the center of the disk,\* the chromospheric faculae stand out all over the disk.

The magnetic features are often found in specific configurations, such as *active regions*. At its maximum development, a large active region contains a group of sunspots and faculae. The faculae are arranged in *plages* and in an irregular network, called the *enhanced network*. The term *plage* indicates a tightly knit, coherent distribution of faculae; the term is inspired by the appearance in filtergrams recorded in one of the line cores of the Ca II resonance lines (see Figs. 1.1*b* and 1.3*a*). *Enhanced network* stands out in

\* Some of the drawings in Father Schreiner’s (1630) book show faculae near disk center.



1.1 *b*

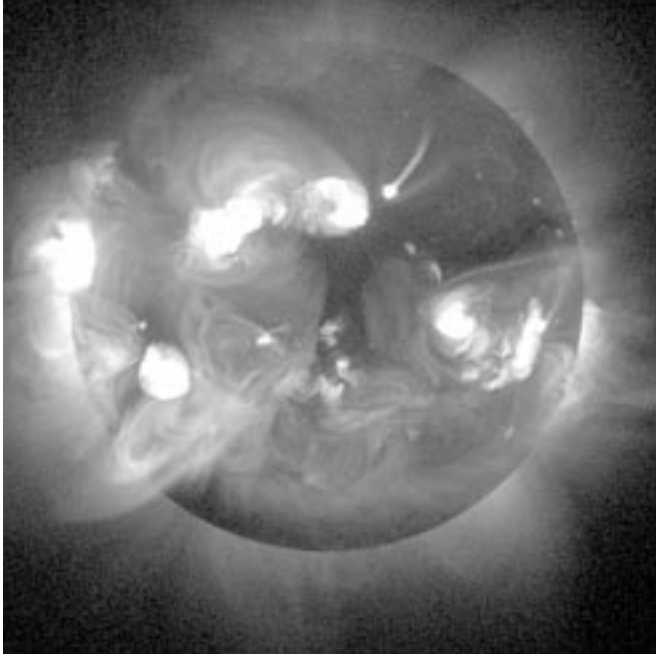


1.1 *c*

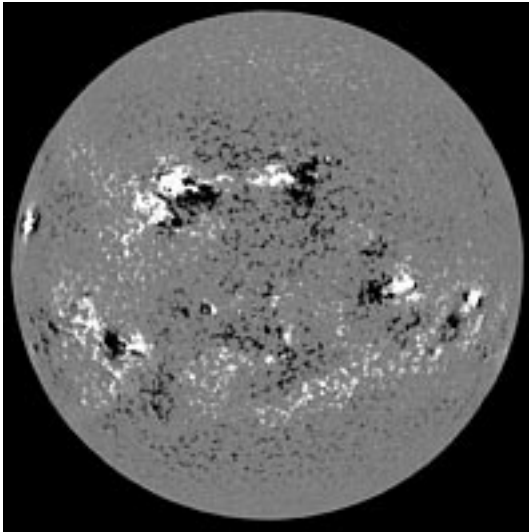
Figs. 1.2*b* and 1.2*c*. All active regions, except the smallest, contain (a group of) sunspots or pores during the first part of their evolution.

Active regions with sunspots are exclusively found in the *sunspot belts* on either side of the solar equator, up to latitudes of  $\sim 35^\circ$ ; the panels in Fig. 1.1 show several large active regions. In many young active regions, the two magnetic polarities are found in a nearly E–W bipolar arrangement, as indicated by the magnetogram of Fig. 1.1*e*, and better in the orientations of the sunspot groups in Fig. 1.1*a*. Note that on the northern solar hemisphere in Fig. 1.1*e* the western parts of the active regions tend to be of negative

4 *Introduction: solar features and terminology*



1.1 *d*



1.1 *e*

polarity, whereas on the southern hemisphere the western parts are of positive polarity. This polarity rule, discovered by G. E. Hale, is discussed in Section 6.1.

Since many active regions emerge close to or even within existing active regions or their remnants, the polarities may get distributed in a more irregular pattern than a simple bipolar arrangement. Such a region is called a complex active region, or an *activity complex*. Figure 1.2 portrays a mildly complex active region.

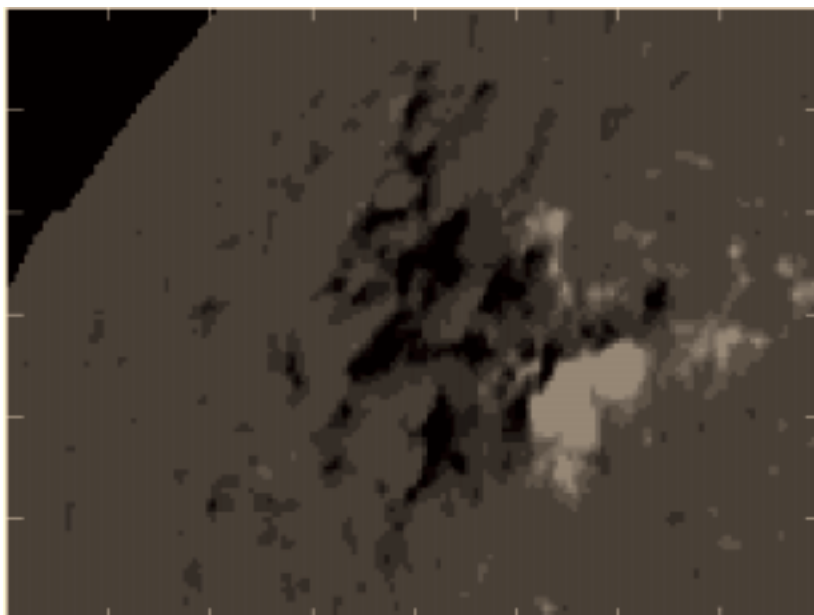
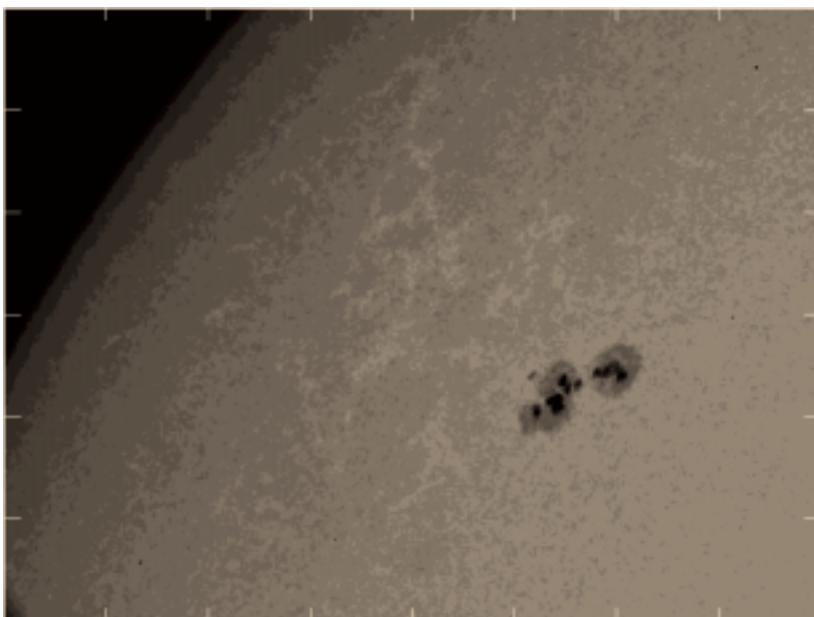
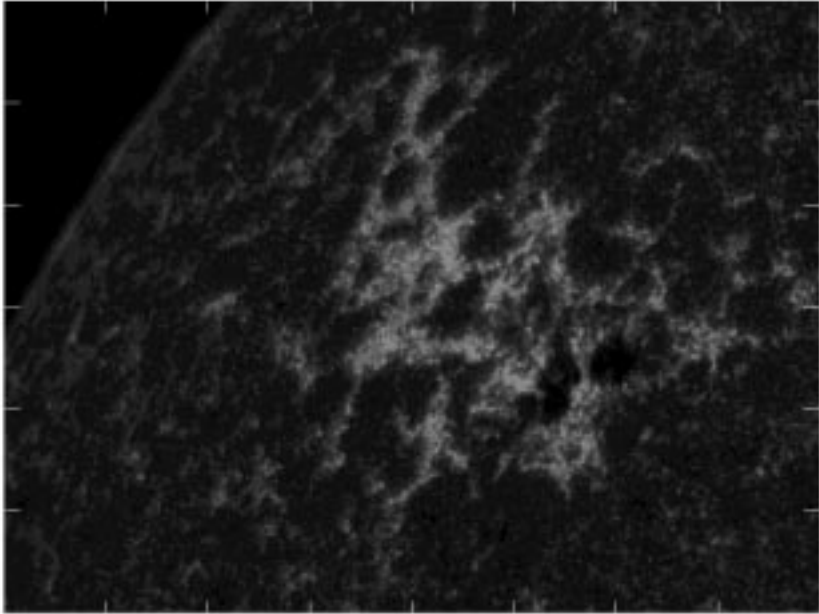
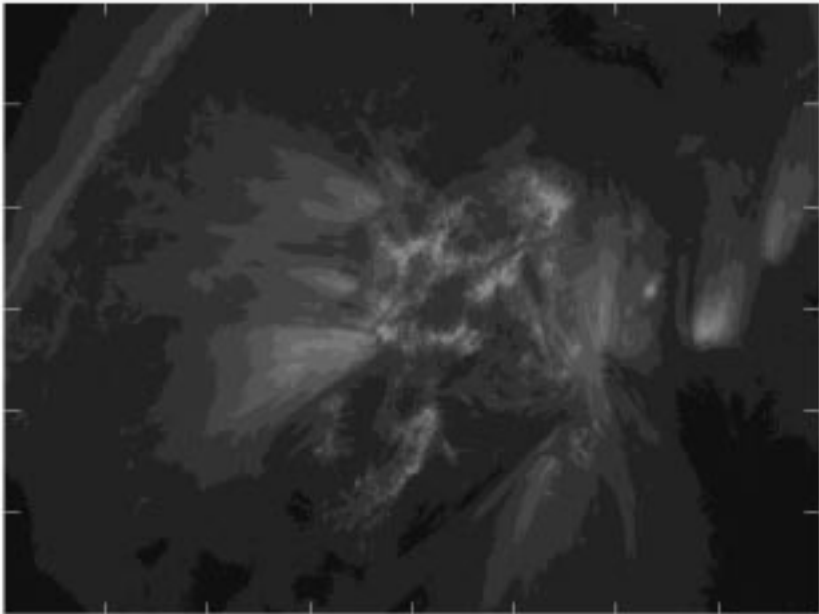
1.2 *a*1.2 *b*

Fig. 1.1. Complex active region AR 8,227 observed on 28 May 1998 around 12 UT in various spectral windows. Panels: *a*, magnetogram (NSO-Kitt Peak); *b*, in white light (*TRACE*); *c*, in a 100-Å band centered at  $\sim 1,550$  Å, showing the continuum emission from the high photosphere and CIV transition-region emission (*TRACE*); *d*, at 171 Å, dominated by spectral lines of Fe IX and Fe X, with a peak sensitivity at  $T \approx 1$  MK (*TRACE*).



1.2 c



1.2 d

When a large active region decays, usually first the sunspots disappear, and then the plages crumble away to form enhanced network. One or two stretches of enhanced network may survive the active region as a readily recognizable bipolar configuration. Stretches of enhanced network originating from several active regions may combine into one large strip consisting of patches of largely one dominant polarity, a so-called unipolar region. On the southern hemisphere of Fig. 1.1*e*, one such strip of enhanced network of positive (white) polarity stands out. Enhanced network is a conspicuous configuration on the solar disk when activity is high during the sunspot cycle.

Outside active regions and enhanced network, we find a *quiet network* that is best visible as a loose network of small, bright mottles in Ca II K filtergrams and in the UV continuum. Surrounding areas of enhanced network and plage in the active complex, the quiet network is indicated by tiny, bright mottles; see Fig. 1.2*c*. Quiet network is also visible on high-resolution magnetograms as irregular distributions of tiny patches of magnetic flux of mixed polarities. This mixed-polarity quiet network is the configuration that covers the solar disk everywhere outside active regions and their enhanced-network remnants; during years of minimum solar activity most of the solar disk is dusted with it. The areas between the network patches are virtually free of strong magnetic field in the photosphere; these areas are often referred to as internetwork cells. Note that in large parts of the quiet network, the patches are so widely scattered that a system of cells cannot be drawn unambiguously.

The distinctions between plages, enhanced network, and quiet network are not sharp. Sometimes the term *plagette* is used to indicate a relatively large network patch or a cluster of faculae that is too small to be called plage.

Bright chromospheric mottles in the quiet network are usually smaller than faculae in active regions and mottles in enhanced network, but otherwise they appear similar. Historically, the term *facula* has been reserved for bright mottles within active regions; we call the bright mottles outside active regions *network patches*. (We prefer the term patch over point or element, because at the highest angular resolution these patches and faculae show a fine structure.)

The comparison between the magnetograms and the photospheric and chromospheric images in Figs. 1.1 and 1.1 shows that near the center of the solar disk there is an unequivocal relation between sites of strong, vertical magnetic field and sunspots, faculae, and network patches. As a consequence, the adjectives magnetic and chromospheric are used interchangeably in combination with faculae, plages, and network.

In most of the magnetic features, the magnetic field is nearly vertical at the photospheric level, which is one of the reasons for the sharp drop in the line-of-sight magnetic signal in plages and network toward the solar limb in Fig. 1.1*e*. Markedly inclined photospheric fields are found within tight bipoles and in sunspot penumbrae.

Filtergrams obtained in the core of H $\alpha$  are much more complex than those in the Ca II H and K lines (see Fig. 1.3, and Zirin's 1988 book, which is full of them). In addition to plages and plagettes consisting of bright mottles, they show a profusion of elongated dark fibrils. These fibrils appear to be directed along inclined magnetic field lines in the upper chromosphere (Section 8.1); they are rooted in the edges of plages and in the network patches. The fibrils stand out particularly well in filtergrams obtained at  $\sim 0.5 \text{ \AA}$  from the line core (see Fig. 1.3*b*).

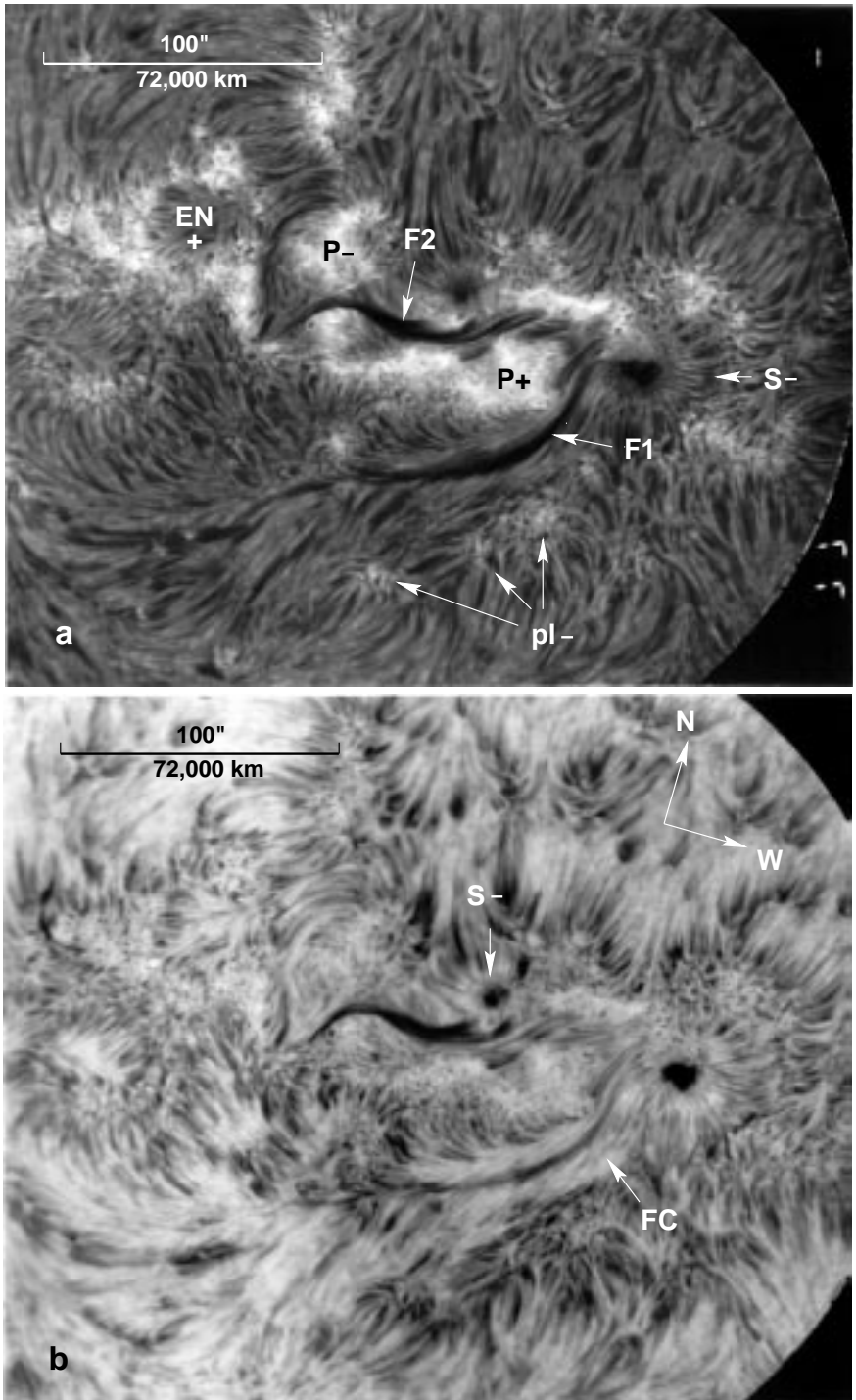


Fig. 1.3. Nearly simultaneous  $H\alpha$  filtergrams of active complex McMath 14,726 on 18 April 1977, observed in the line core (panel *a*) and at  $\Delta\lambda = +0.65 \text{ \AA}$  in the red wing (panel *b*). The letter symbols indicate the following: S, sunspot; P, plage; pl, plagette; F, filament; FC, filament channel; EN, enhanced network cell. Signs are appended to indicate the magnetic polarities. Fibrils are prominent in both panels. Exceptionally long and well-ordered fibrils are found in the northwestern quadrants. Several features are discussed in Sections 8.1 and 8.2. The chirality of filament F1 is sinistral (figure from the archive of the Ottawa River Solar Observatory, National Research Council of Canada, courtesy of V. Gaizauskas.)

The longest dark structures visible in the core of the  $H\alpha$  line are the *filaments* (Figs. 1.1c and 1.3). Many filaments are found at borders of active regions and within active complexes, but there are also filaments outside the activity belts, at higher latitudes. Most filaments differ from fibrils by their length and often also by their detailed structure. Small filaments can be distinguished from fibrils by their reduced contrast at distances  $|\Delta\lambda| \gtrsim 0.5 \text{ \AA}$  from the line core. Large filaments are visible outside the solar limb as *prominences* that are bright against a dark background.

The *corona* is the outermost part of the Sun, which is seen during a total eclipse as a pearly white, finely structured halo, locally extending to several solar radii beyond the photospheric limb; see Figs. 8.4 and 8.11, Fig. 1.2 in Golub and Pasachoff (1997), or Fig. 9-10 in Foukal (1990). The coronal plasma is extremely hot ( $T \sim 1 \times 10^6 - 5 \times 10^6 \text{ K}$ ) and tenuous. The radiation of the white-light corona consists of photospheric light, scattered by electrons in the corona and by interplanetary dust particles; the brightness of the inner corona is only  $\sim 10^{-6}$  of the photospheric brightness. The thermal radiation of the corona is observed in soft X-rays, in spectral lines in the ultraviolet and optical spectrum, and in radio waves. The corona is optically thin throughout the electromagnetic spectrum, except in radio waves and a few resonance lines in the extreme ultraviolet and in soft X-rays.

The coronal structure in front of the photospheric disk can be observed from satellites in the EUV and in X-rays; see Figs. 1.1d and 1.2d. In these wavelength bands, the coronal plasma, however optically thin, outshines the much cooler underlying photosphere. The features depend on the magnetic field in the underlying photosphere. The corona is particularly bright in “coronal condensations” immediately above all active regions in the photosphere and chromosphere. Coronal loops trace magnetic field lines connecting opposite polarities in the photosphere. Note that in Fig. 1.1d there are also long, somewhat fainter, loops that connect magnetic poles in different active regions. The finest coronal structure is displayed in Fig. 1.2d, where the passband reveals radiation from bottom parts of loops with  $T \lesssim 1 \times 10^6 \text{ K}$ , without contamination by radiation from hotter loops with  $T \gtrsim 2 \times 10^6 \text{ K}$ .

*Coronal holes* stand out as regions that emit very little radiation; these have been identified as regions where the magnetic field is open to interstellar space. Usually large coronal holes are found over the polar caps; occasionally smaller coronal holes are observed at low latitudes.